

Triviality and the Higgs mass lower bound

K. Holland^{a*}

^aDept. of Physics, University of California San Diego, 9500 Gilman Drive, La Jolla CA 92093-0319, USA

In the minimal Standard Model, it is commonly believed that the Higgs mass cannot be too small, otherwise Top quark dynamics makes the Higgs potential unstable. Although this Higgs mass lower bound is relevant for current phenomenology, we show that the Higgs vacuum instability in fact does not exist and only appears when treating incorrectly the cut-off in the renormalization of a trivial theory. We also demonstrate how to calculate correctly the regulator-dependent Higgs mass lower bound.

1. VACUUM INSTABILITY

In this talk I report on some recent work which was done in collaboration with Julius Kuti [1]. The as-yet unobserved Higgs boson plays a crucial role in determining the threshold of new physics beyond the Standard Model (SM). Precision Electroweak measurements indicate that, if the SM is correct, the Higgs is light with a mass $m_{\text{Higgs}} = 114_{-45}^{+69}$ GeV [2]. Even if one excludes these experimental constraints, it is widely believed on theoretical grounds that the Higgs mass must lie within a certain range for the SM to be an acceptable field theory. Fig. 1 shows the current phenomenological upper and lower m_{Higgs} bounds as a function of Λ , the energy scale at which physics beyond the SM must set in [3]. Upper and lower bounds are very important for two reasons. Firstly, they tell us where we should look for the Higgs. For example, according to Fig. 1, the SM cannot sustain a Higgs as heavy as 1 TeV. Secondly and more importantly, if the Higgs is observed, knowing its mass would tell us the maximum energy scale up to which the SM can be valid. According to this plot, the lower bound is the relevant one for current phenomenology. For example, taking the preferred value $m_{\text{Higgs}} = 114$ GeV, the SM is at most valid up to around 100 – 1000 TeV. The phenomenological lower bound is based on the instability of the Higgs potential if m_{Higgs} is too small. We will

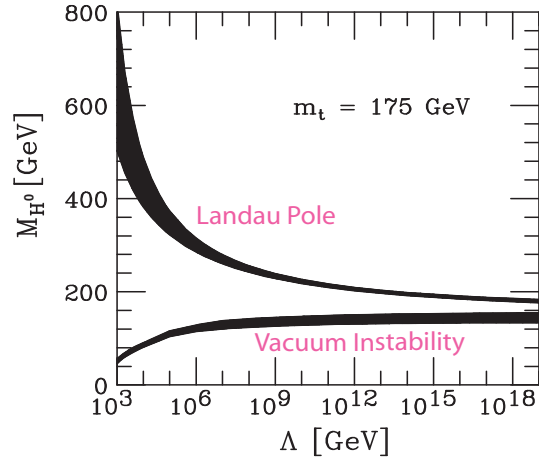


Figure 1. Upper and lower SM m_{Higgs} bounds [3].

show that this vacuum instability, like the Landau pole, is fake. Remarkably, just like the upper bound, a new regulator-dependent lower bound emerges from the triviality of the theory. An earlier version of this work was presented in [4].

The apparent vacuum instability can be seen in a Higgs-Yukawa model of a single real scalar field (Higgs) coupled to N_F degenerate fermions (Top quarks). The 1-loop Higgs effective potential U_{eff} is calculated by summing an infinite series of di-

*Research supported by the DOE under grant DOE-FG03-97ER40546.

agrams, giving

$$\begin{aligned}
 U_{\text{eff}} &= V + 1/2 \int_k \ln[k^2 + V''] \\
 &\quad - 2N_F \int_k \ln[k^2 + y^2 \Phi^2], \\
 V &= m^2 \Phi^2/2 + \lambda \Phi^4/24.
 \end{aligned}
 \tag{1}$$

The fermion contribution is negative, due to the minus sign associated with every fermion loop. Regulating the integrals and adding counterterms to absorb the divergences in the normal fashion, the renormalized effective potential is

$$\begin{aligned}
 U_{\text{eff}} &= V + \{(V'')^2/64\pi^2\} \{\ln[V''/\mu^2] - 3/2\} \\
 &\quad - \{N_F y^4 \Phi^4/16\pi^2\} \{\ln[y^2 \Phi^2/\mu^2] - 3/2\}.
 \end{aligned}
 \tag{2}$$

For Φ large, the negative fermion contribution dominates if $\lambda^2 < 16N_F y^4$ and the potential appears unstable, it no longer has its ground state at $\Phi = v$. For fixed Yukawa coupling y (i.e. m_{Top}/v), if we require that U_{eff} be stable, this gives a lower bound for λ and hence m_{Higgs} (at tree-level the relation is $\lambda = 3m_{\text{Higgs}}^2/v^2$) [5].

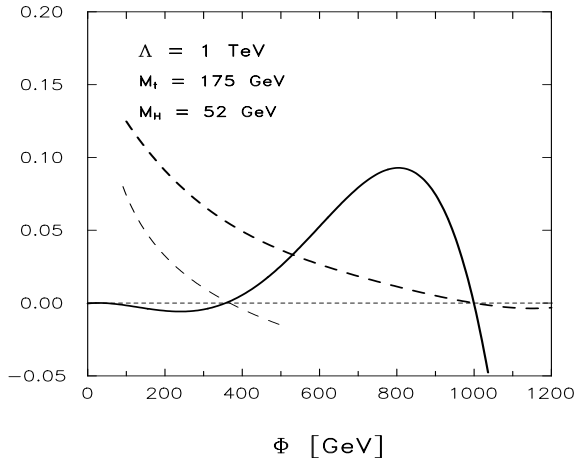


Figure 2. Higgs potential (solid line) and $\lambda(\mu = \alpha\Phi)$ (thick dashed line) for $m_{\text{Higgs}} = 52$ GeV [6].

To eliminate the large logs in Eq. 2, the RG-improved Higgs effective potential in the Stan-

dard Model has been calculated to two loops [6,7]. Fig. 2 shows this effective potential for a particular choice of m_{Top} and m_{Higgs} . If Fig. 2 were representing the true behavior in the SM for $m_{\text{Higgs}} = 52$ GeV, the ground state at $\Phi = v = 246$ GeV could be preserved only by changes in the shape of U_{eff} from new physics beyond the SM around $\Phi \sim 1$ TeV. If m_{Higgs} is increased, the scale of the required new physics is also increased as shown in Fig. 1. Fig. 2 also shows the running coupling $\lambda(\mu = \alpha\Phi)$. For a particular choice of α , the instability of the potential coincides with $\lambda(\mu = \alpha\Lambda) = 0$. The lower bound in Fig. 1 is the smallest m_{Higgs} value such that the instability appears at $\Phi = \Lambda$. The finite thickness of the lower bound is an estimate of the uncertainty of the theoretical calculation. In a renormalizable field theory, one expects that this uncertainty can, in principle, be reduced.

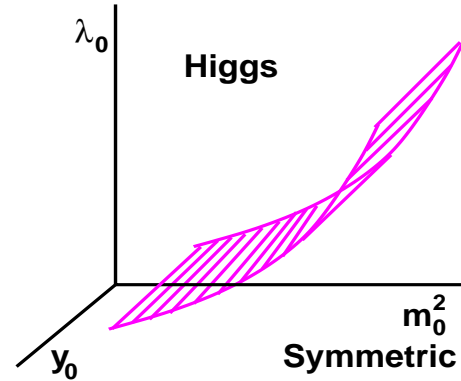


Figure 3. Phase diagram of Higgs-Yukawa model.

2. VACUUM IS STABLE

The effective potential U_{eff} can be calculated non-perturbatively via lattice simulations as shown by Kuti and Shen [8]. We will concentrate on the Higgs-Yukawa model of one real scalar field coupled to N_F degenerate fermions. Fig. 3 shows

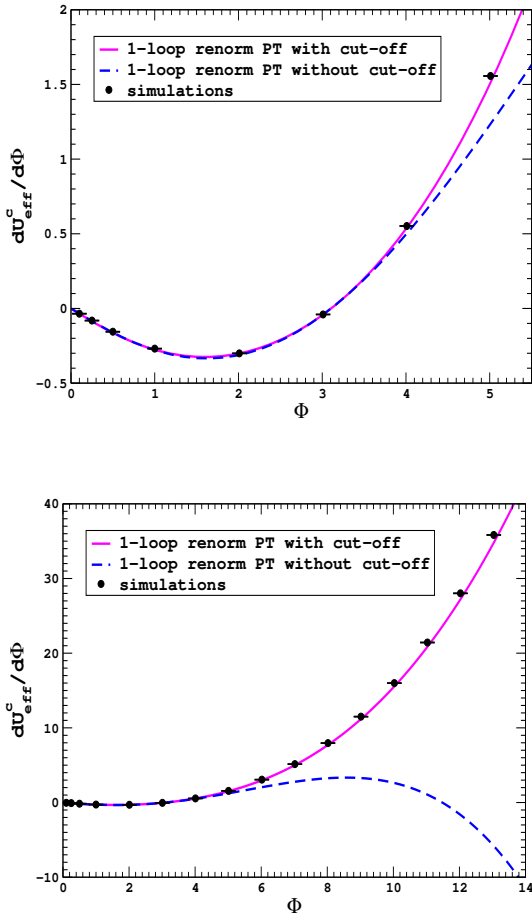


Figure 4. $dU_{\text{eff}}^c/d\Phi$ shown on two different scales.

the phase diagram of the lattice-regulated theory as a function of the bare couplings λ_0 , y_0 and m_0^2 . The lattice spacing is a and the cut-off of the theory is $\Lambda = \pi/a$, the maximum-allowed momentum. The Higgs and symmetric phases are separated by a critical surface where the vacuum expectation value and physical masses vanish, $va, m_{\text{ph}}a \rightarrow 0$ (all dimensionful quantities are calculated in lattice-spacing units). Close to the critical surface on the Higgs side, $\Lambda/m_{\text{ph}} = \pi/m_{\text{ph}}a$ and $\xi/a = 1/m_{\text{ph}}a$ are large (ξ is the correlation length) and the theory is very close to the contin-

uum limit where the cut-off is sent to infinity. In this scaling region, effects due to the finite cut-off are expected to be small.

For a given action $S[\phi]$, the constraint effective potential U_{eff}^c in a finite volume Ω is

$$\exp(-\Omega U_{\text{eff}}^c(\Phi)) = \int [D\phi] \delta(\Phi - 1/\Omega \sum_x \phi(x)) \cdot \exp(-S[\phi]), \quad (3)$$

where the delta-function constrains the average of ϕ to a fixed value Φ . The constraint effective potential U_{eff}^c has an absolute minimum at non-zero Φ in the Higgs phase even at finite volume Ω , as the constraint potential is not convex [9]. This allows the Higgs and symmetric phases to be clearly distinguished at finite volume.

We examine the Higgs-Yukawa model with 2 flavors of staggered lattice fermions (this corresponds to $N_F = 8$ fermions in the continuum limit). The derivative of the constraint effective potential is

$$\begin{aligned} dU_{\text{eff}}^c/d\Phi &= m_0^2 \Phi + 1/6 \lambda_0 \langle \phi^3 \rangle_{\Phi} \\ &\quad - 2y_0 \langle \text{Tr}(D^{-1}[\phi]) \rangle_{\Phi}, \end{aligned} \quad (4)$$

where D is the Dirac operator and $\langle \dots \rangle_{\Phi}$ denotes expectation values where $\Phi = 1/\Omega \sum_x \phi(x)$ is held fixed. In Fig. 4 we plot $dU_{\text{eff}}^c/d\Phi$ for a particular choice of bare couplings in the Higgs phase. From the lattice simulations, we see that $dU_{\text{eff}}^c/d\Phi$ vanishes at $\Phi = 0$ (a local maximum) and $\Phi \approx 3.1$ (the absolute minimum). There is no indication that the potential becomes unstable at large Φ .

We also compare the results of the simulations with 1-loop renormalized perturbation theory. Adding explicitly the counterterms and keeping the cut-off Λ finite, the 1-loop constraint effective potential is

$$\begin{aligned} U_{\text{eff}}^c &= V + 1/2 \int_{k \neq 0}^{\Lambda} \ln[1 + V''/k^2] \\ &\quad - 2N_F \int_{k \neq 0}^{\Lambda} \ln[1 + y^2 \Phi^2/k^2] \\ &\quad - 1/2 \int_{k \neq 0}^{\Lambda} \{V''/k^2 - (V'')^2/2[k^2 + \mu^2]^2\} \\ &\quad + 2N_F \int_{k \neq 0}^{\Lambda} \{y^2 \Phi^2/k^2 - y^4 \Phi^4/2[k^2 + \mu^2]^2\}. \end{aligned} \quad (5)$$

Naively taking the cut-off $\Lambda \rightarrow \infty$ gives the continuum effective potential as in Eq. 2. In Fig. 4 we see that for small Φ , continuum renormalized perturbation theory agrees well with the simulation results, even though the cut-off is naively sent to infinity. However for larger Φ , continuum perturbation theory incorrectly predicts that the ground state is unstable. In contrast, renormalized perturbation theory *with a finite cut-off* is in perfect agreement with the non-perturbative simulation results for all values of Φ . The ground state of the theory is in fact stable.

3. TRIVIALITY

The Higgs potential only appears unstable when the cut-off is incorrectly sent to infinity. The standard renormalization procedure of adding counterterms and removing the cut-off fails in a trivial theory. A quantum field theory is defined by a set of bare couplings and a regulator. A theory is trivial if the renormalized couplings vanish when the regulator is removed, for any choice of bare couplings. In this situation, the cut-off must remain finite to have a non-trivial interacting theory.

We will show how standard renormalization fails in the trivial Higgs-Yukawa model in the large- N_F limit. In terms of the bare fields and couplings, the Lagrangian is

$$\begin{aligned}
\mathcal{L} &= m_0^2 \phi_0^2/2 + \lambda_0 \phi_0^4/24 + y_0 \phi_0 \bar{\Psi}_0^a \Psi_0^a + \text{K.E.} \\
&= m_0^2 Z_\phi^2 \phi^2/2 + \lambda_0 Z_\phi^2 \phi^4/24 \\
&+ y_0 Z_\phi^{1/2} Z_\Psi \phi \bar{\Psi}^a \Psi^a + \text{K.E.} \\
&= (m^2 + \delta m^2) \phi^2/2 + (\lambda + \delta \lambda) \phi^4/24 \\
&+ (y + \delta y) \phi \bar{\Psi}^a \Psi^a + \text{K.E.} \tag{6}
\end{aligned}$$

where $a = 1, \dots, N_F$, $\phi_0 = Z_\phi^{1/2} \phi$, $\Psi_0 = Z_\Psi^{1/2} \Psi$ and δm^2 , $\delta \lambda$ and δy are the counterterms. In the limit $N_F \rightarrow \infty$, only Feynman diagrams with fermion loops contribute, hence $Z_\Psi = 1$. The bare and renormalized couplings are related as

$$\begin{aligned}
m_0^2 Z_\phi^2 &= m^2 + \delta m^2, & \lambda_0 Z_\phi^2 &= \lambda + \delta \lambda, \\
y_0 Z_\phi^{1/2} &= y + \delta y, \tag{7}
\end{aligned}$$

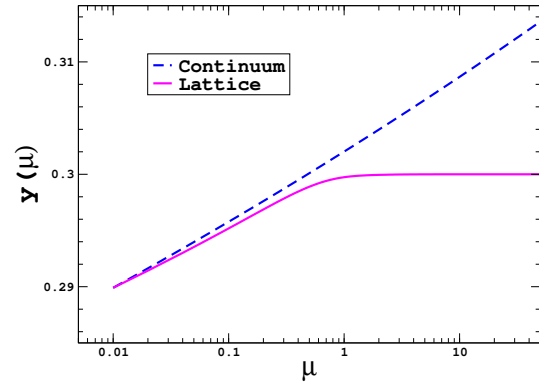
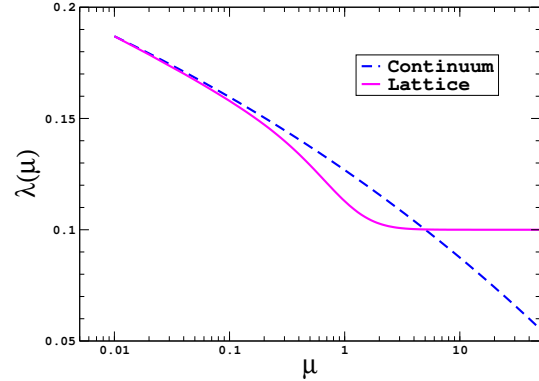


Figure 5. Renormalized couplings $\lambda(\mu)$ and $y(\mu)$.

where the counterterms are

$$\begin{aligned}
\delta m^2 &= 4N_F y^2 \int_k^\Lambda 1/k^2, \\
\delta y &= 0, \\
\delta \lambda &= -24N_F y^4 \int_k^\Lambda 1/[k^2 + \mu^2]^2, \tag{8}
\end{aligned}$$

and the wave-function renormalization is

$$\begin{aligned}
G_\phi^{-1}(p^2) &= p^2 + m_{\text{Higgs}}^2 - \Sigma(p^2), \\
Z_\phi^{-1} &= dG_\phi^{-1}/dp^2|_{p^2=0}, \\
\Sigma(p^2) &= -4N_F y^2 \int_k^\Lambda [\mu^2 - k \cdot (k - p)] / \\
&\quad \{[k^2 + \mu^2][(k - p)^2 + \mu^2]\}. \tag{9}
\end{aligned}$$

Note that we keep the regulator cut-off Λ finite. The bare couplings and physical predictions are independent of the renormalization group scale μ . Keeping the bare couplings fixed, we vary the RG scale μ and use Eq. 7 to determine the RG flow of the renormalized couplings $m^2(\mu)$, $\lambda(\mu)$ and $y(\mu)$.

In Fig. 5 we plot the RG flow of $\lambda(\mu)$ and $y(\mu)$ using a lattice regulator for the integrals and with the arbitrary choice $\lambda_0 = 0.1, y_0 = 0.3$. The RG scale μ is in lattice-spacing units. When the RG scale is much lower than the cut-off ($\mu \ll 1$), the renormalized couplings flow exactly as predicted by the continuum large- N_F RG equations

$$\begin{aligned} y^2(\mu) &= y_1^2/[1 - (N_F y_1^2/4\pi^2) \ln \mu] \\ \lambda(\mu) &= 12y^2(\mu) + c_1 y^4(\mu). \end{aligned} \quad (10)$$

In the limit where the cut-off is infinite, $\mu \rightarrow 0$ and the renormalized couplings $y(\mu)$ and $\lambda(\mu)$ vanish. As we said, the theory is trivial, with no interaction when the regulator is removed. In this regime ($\mu \ll 1$), continuum renormalized perturbation theory is perfectly valid, as the effects of the finite cut-off are negligible. When the RG scale is close to the cut-off ($\mu \sim 1$), the true RG flow of the couplings deviates from the continuum prediction. As μ increases, continuum perturbation theory predicts that $\lambda(\mu)$ becomes negative — this is the vacuum instability. However for $\mu \gg 1$, Eqs. 8 and 9 show that $\delta\lambda \rightarrow 0$ and $Z_\phi \rightarrow 1$. The renormalized couplings actually flow to the bare values $\lambda(\mu) \rightarrow \lambda_0, y(\mu) \rightarrow y_0$, exactly as shown in Fig. 5. The continuum prediction that $\lambda(\mu)$ turns negative and the potential becomes unstable is incorrect, because the cut-off dependence of the true RG flow has been neglected.

4. TRUE HIGGS LOWER BOUND

The widely-accepted m_{Higgs} lower bound of Fig. 1 is based on a vacuum instability appearing if the Higgs is too light. Using non-perturbative lattice calculations, perturbation theory, and the large- N_F limit, we see that there is no vacuum instability. The theory is trivial and the cut-off must be kept finite for the renormalized couplings not to vanish. The effective potential only appears unstable when the cut-off dependence of the

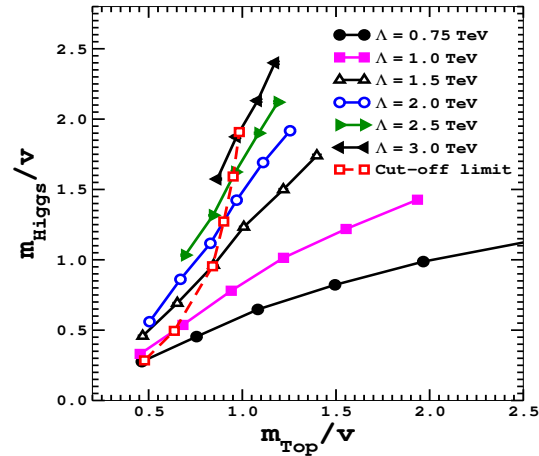
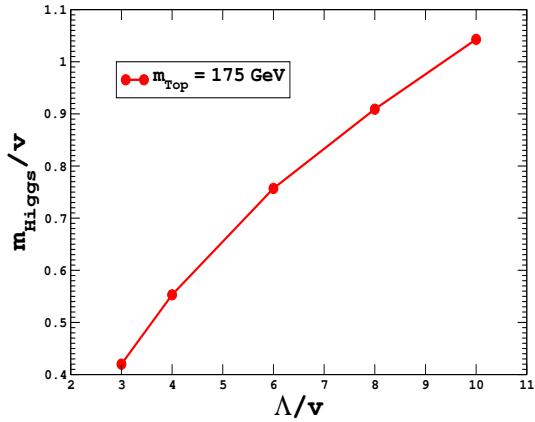


Figure 6. Summary of lattice simulation results.

renormalization procedure is ignored.

If there is no vacuum instability, is there an m_{Higgs} lower bound? As the theory is trivial, we require a finite cut-off to have a non-trivial interaction. In the Higgs phase of the theory very close to the critical surface (as shown in Fig. 3), the cut-off is finite but large. For a fixed cut-off, upper and lower bounds for m_{Higgs} can be determined by exploring all allowed bare couplings [10]. Moving away from the critical surface, the cut-off decreases and at some point the theory is completely dominated by cut-off effects and ceases to be physically acceptable.

We have used non-perturbative lattice simulations to explore the phase diagram of the Higgs-Yukawa model with a single real scalar field coupled to 2 flavors of staggered fermions ($N_F = 8$ continuum flavors). In Fig. 6 we display a summary of the results. All quantities are calculated in units of the lattice spacing a . For illustrative purposes, the cut-off $\Lambda = \pi/a$ is converted into physical units using the Standard Model value $v = 246$ GeV. For example, $va = 0.2$ corresponds to $\Lambda/v = \pi/0.2$ i.e. $\Lambda \sim 4$ TeV. For fixed m_{Top} and Λ , we find that the smallest Higgs mass is generated when the bare Higgs coupling $\lambda_0 \rightarrow 0$.

Figure 7. Lower bound for $m_{\text{Top}} = 175$ GeV.

The bare Higgs coupling cannot be negative, otherwise the theory is not defined, as all functional integrals diverge. The solid curves in Fig. 6 correspond to $\lambda_0 = 0$ and Λ fixed in physical units (with three bare parameters and two constraints, this leaves one degree of freedom). With a finite cut-off, one must keep track of the finite cut-off effects. We use the ad hoc definition $m_{\text{ph}a} = 0.5$, applied to both Higgs and Top masses, as the smallest allowed correlation length, corresponding to the dashed line in Fig. 6. To the left of the dashed line, we expect the cut-off effects to be reasonably small and the theory to be physically acceptable. A similar constraint was used by Lüscher and Weisz for the $O(4)$ Higgs sector, where the violation of rotational symmetry in Goldstone-boson scattering was investigated [11].

Interpolating the results sketched in Fig. 6 we can extract the Higgs mass lower bound as a function of the cut-off for fixed physical Top mass. The curve in Fig. 7 corresponds to the Higgs lower bound at $m_{\text{Top}} = 175$ GeV. It is quite natural that the Higgs lower bound is attained when the bare Higgs coupling $\lambda_0 = 0$. Previous studies of the pure Higgs $\lambda\phi^4$ theory showed that the m_{Higgs} upper bound is reached when $\lambda_0 = \infty$ [12].

One important consideration is that the lower bound is regulator-dependent. Consider the

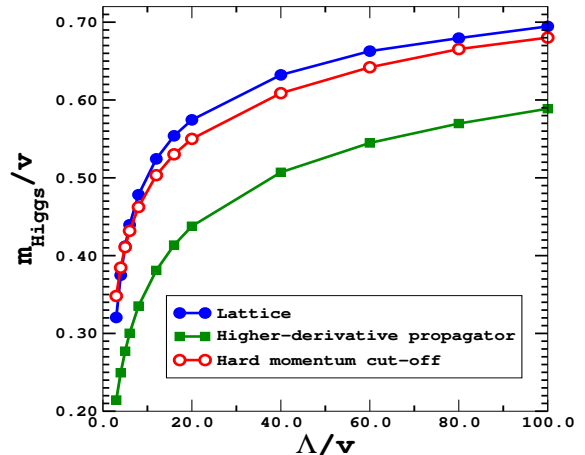


Figure 8. Regulator-dependence of lower bound.

$N_F \rightarrow \infty$ limit of the Higgs-Yukawa model, where perturbation theory becomes exact. We compare the Higgs lower bound, calculated using three different regulators: a hard cut-off in the momentum integration, a lattice regulator, and a higher-derivative propagator $k^2 \rightarrow k^2(1 + k^2/\Lambda^2)^2$. In Fig. 8 we plot the Higgs lower bound for a fixed Top mass. Even when the cut-off is quite large, the lower bound varies by as much as 20% among these three regulators. This is a feature of trivial theories which cannot be ignored — when the cut-off is finite, not all quantities are universal. For any given regulator, one can calculate the Higgs lower bound to whatever desired accuracy. However, one cannot make arbitrarily accurate predictions which are regulator-independent. There is an inherent ambiguity in the bound and one can at best estimate the energy scale where the theory is no longer physically acceptable.

5. PROPOSAL

We have examined a toy Higgs-Yukawa model of one real scalar field coupled to N_F degenerate fermions. Earlier studies of Higgs-Yukawa models were reported in [13]. To make a quantitative statement relevant for the Standard Model, one

needs to study a more physical model. A realistic approximation would be an $SU(2)$ Higgs doublet (corresponding to an $O(4)$ -symmetric scalar field) coupled to a single fermion flavor (the Top quark). Gluons should also be included, as the QCD coupling makes a significant contribution to the RG flow of the Top Yukawa coupling. The remaining degrees of freedom of the Standard Model are expected to play a negligible role in the lower bound. If it is only possible to calculate the lower bound via lattice simulations, a gluon-Higgs-Top model is a very challenging system to explore. The only completely satisfactory way to represent a single massless fermion flavor on the lattice is to use a chiral Ginsparg-Wilson fermion [14], which is computationally very demanding. Coupled to fluctuating scalar fields, the positivity of the fermion determinant in the functional integral is not guaranteed, and must be examined in the Higgs phase of the theory. If the probability distribution in the functional integral can be negative, this could make numerical computations very difficult (the so-called Sign problem). This is analogous to the situation in lattice QCD and how light a quark mass is possible in practical numerical simulations, which is very sensitive to the nature of the lattice fermion. Despite these challenges, we believe a realistic lattice study of a gluon-Higgs-Top system can make a significant and timely contribution to current tests of the Standard Model.

REFERENCES

1. K. Holland and J. Kuti, in preparation.
2. LEP Electroweak Working Group 2004-08.
3. K. Hagiwara *et al.* [Particle Data Group Collaboration], Phys. Rev. D **66**, 010001 (2002).
4. K. Holland and J. Kuti, Nucl. Phys. Proc. Suppl. **129**, 765 (2004).
5. I. V. Krive and A. D. Linde, Nucl. Phys. B **117**, 265 (1976); H. D. Politzer and S. Wolfram, Phys. Lett. B **82**, 242 (1979); N. Cabibbo, L. Maiani, G. Parisi and R. Petronzio, Nucl. Phys. B **158**, 295 (1979); M. Sher, Phys. Rept. **179**, 273 (1989); C. Ford, D. R. T. Jones, P. W. Stephenson and M. B. Einhorn, Nucl. Phys. B **395**, 17 (1993).
6. J. A. Casas, J. R. Espinosa and M. Quiros, Phys. Lett. B **382**, 374 (1996).
7. G. Altarelli and G. Isidori, Phys. Lett. B **337**, 141 (1994).
8. J. Kuti and Y. Shen, Phys. Rev. Lett. **60**, 85 (1988).
9. L. O’Raifeartaigh, A. Wipf and H. Yoneyama, Nucl. Phys. B **271**, 653 (1986).
10. R. F. Dashen and H. Neuberger, Phys. Rev. Lett. **50**, 1897 (1983).
11. M. Lüscher and P. Weisz, Nucl. Phys. B **318**, 705 (1989).
12. J. Kuti, L. Lin and Y. Shen, Phys. Rev. Lett. **61**, 678 (1988); G. Bhanot and K. Bitar, Phys. Rev. Lett. **61**, 798 (1988); U. M. Heller, M. Klomfass, H. Neuberger and P. Vranas, Nucl. Phys. B **405**, 555 (1993); P. Hasenfratz and J. Nager, Z. Phys. C **37**, 477 (1988); A. Hasenfratz, K. Jansen, C. B. Lang, T. Neuhaus and H. Yoneyama, Phys. Lett. B **199**, 531 (1987); M. Lüscher and P. Weisz, Phys. Lett. B **212**, 472 (1988).
13. L. Lin, I. Montvay, G. Munster, M. Plagge and H. Wittig, Phys. Lett. B **317**, 143 (1993); W. Bock, C. Frick, J. Smit and J. C. Vink, Nucl. Phys. B **400**, 309 (1993); I. H. Lee, J. Shigemitsu and R. E. Shrock, Nucl. Phys. B **330**, 225 (1990); Y. Shen, J. Kuti, L. Lin and P. Rossi, Nucl. Phys. Proc. Suppl. **9**, 99 (1989); Y. Shen, Nucl. Phys. Proc. Suppl. **20**, 613 (1991).
14. P. H. Ginsparg and K. G. Wilson, Phys. Rev. D **25**, 2649 (1982); P. Hasenfratz, Nucl. Phys. B **525**, 401 (1998); P. Hasenfratz and F. Niedermayer, Nucl. Phys. B **414**, 785 (1994); P. Hasenfratz *et al.*, Nucl. Phys. B **643**, 280 (2002); C. Gattringer *et al.*, Nucl. Phys. B **677**, 3 (2004); D. B. Kaplan, Phys. Lett. B **288**, 342 (1992); Y. Shamir, Nucl. Phys. B **406**, 90 (1993); V. Furman and Y. Shamir, Nucl. Phys. B **439**, 54 (1995); T. Blum *et al.*, Phys. Rev. D **69**, 074502 (2004); R. Narayanan and H. Neuberger, Nucl. Phys. B **443**, 305 (1995), Nucl. Phys. B **412**, 574 (1994), Phys. Rev. Lett. **71**, 3251 (1993), Phys. Lett. B **302**, 62 (1993).